math xmlns="http://www.w3.org/1998/Math/MathML">mrow>mmultiscripts>mi>Tm/mi>mprescripts>/mprescripts>none>/none>mn>169/mn>/mmultiscripts>mo>(/mo>mi>n/mi>mo>,/mo>mn>2/mn>mi>n/mi>mo>)/mo>mmultiscripts>mi>Tm/mi>mprescripts>/mprescripts>none>/none>mn>168/mn>/mmultiscripts>/mrow>/math> and math xmlns="http://www.w3.org/1998/Math/MathML">mrow>mmultiscripts>mi>Tm/mi>mprescripts>/mprescripts>none>/none>mn>169/mn>/mmultiscripts>mo>(/mo>mi>n/mi>mo>,/mo>mn>3/mn>mi>n/mi>mo>)/mo>mmultiscripts>mi>Tm/mi>mprescripts>/mprescripts>none>/none>mn>167/mn>/mmultiscripts>/mrow>/math> cross-section measurements from 15 to 21 MeV

S. W. Finch, M. Bhike, Krishichayan, J. Soter, and W. Tornow

Phys. Rev. C **103**, 044609 — Published 14 April 2021

DOI: 10.1103/PhysRevC.103.044609

^{169}Tm$(n,2n)^{168}$Tm and ^{169}Tm$(n,3n)^{167}$Tm cross-section measurements from 15 to 21 MeV

S.W. Finch,[1,2,*] M. Bhike,[1,2] Krishichayan,[1,2] J. Soter,[3] and W. Tornow[1,2]

[1]*Department of Physics, Duke University, Durham, NC 27708, USA*
[2]*Triangle Universities Nuclear Laboratory, Durham, NC 27708, USA*
[3]*Thayer School of Engineering, Dartmouth College, Hannover, NH 03755, USA*

(Dated: March 17, 2021)

The ^{169}Tm$(n,2n)^{168}$Tm and ^{169}Tm$(n,3n)^{167}$Tm cross sections have been measured in the neutron energy range between 15 and 21 MeV using the ^{3}H$(d,n)^{4}$He neutron source reaction. The ^{169}Tm$(n,3n)^{167}$Tm data are intended to provide an accurate database for interpreting so-called reaction-in-flight neutron yields, which provide a sensitive tool for studying properties of the deuterium-tritium plasma created in inertial confinement fusion laser shots at the National Ignition Facility at Lawrence Livermore National Laboratory. The data are compared to previous data and evaluations for the reaction studied, and are found to be in good agreement with the ENDF/B-VIII.0 evaluation, although small adjustments are necessary for the ^{169}Tm$(n,3n)^{167}$Tm reaction. For the first time in any $(n,2n)$ cross-section measurements to date, a comprehensive data set ranging from threshold to 21 MeV has been obtained by the same group.

I. INTRODUCTION

The recent interest in the $(n,2n)$ and $(n,3n)$ reactions on ^{169}Tm was triggered by the prospect of using the associated cross-section data as diagnostic tools to better understand the complicated physics governing the deuterium-tritium (DT) inertial confinement fusion (ICF) plasma at the National Ignition Facility (NIF) at Lawrence Livermore National Laboratory. The small DT loaded capsules are positioned at the center of a hohlraum, which when bombarded with powerful lasers at NIF, produces not only 14.1 MeV neutrons via the ^{3}H$(d,n)^{4}$He fusion reaction (in the following also called the DT reaction), but also neutrons of higher energies. Such neutrons can only be created at sufficiently high DT and neutron densities, which will allow deuterons and tritons to obtain enough kinetic energy after neutron elastic scattering within the capsule to initiate the DT reaction at MeV energies rather than at the few keV of energy provided by the X-rays in the hohlraum after a laser shot [1]. These high-energy neutrons are often referred to as reaction-in-flight (RIF) neutrons. Because the fluence of the RIF neutrons with expected maximum energies of close to 30 MeV is many orders of magnitude smaller than that of the primary 14.1 MeV neutrons, it is a challenge to properly detect them. Standard neutron detection methods, including the well-established neutron time-of-flight technique are not applicable at NIF in high-yield laser shots due of the high instantaneous 14.1 MeV neutron flux, creating conditions well beyond the capabilities of even the fasted counting techniques. Therefore, currently only passive methods are suitable for neutron fluence determination in high-yield DT shots at NIF [2]. The ^{169}Tm$(n,2n)^{168}$Tm and ^{169}Tm$(n,3n)^{167}$Tm reactions are important candidates for this approach, which is based on the neutron activation technique. The ^{169}Tm$(n,2n)^{168}$Tm reaction with its threshold energy of 8.1 MeV probes the primary and down-scattered neutron energy spectrum from the ^{3}H$(d,n)^{4}$He reaction, while the ^{169}Tm$(n,3n)^{167}$Tm reaction with its threshold energy of 15.0 MeV can only be initiated by the RIF neutrons. The ratio of RIF neutrons to primary DT neutrons can provide valuable information on the DT plasma density achieved in ICF laser shots, in addition to more subtle effects. See Ref. [3] for more information on this topic. Therefore, it is not surprising that these two reactions have received considerable attention during the past five years, because their cross sections must be known accurately as a function of incident neutron energy in order to provide a sensitive diagnostic tool in ICF plasma studies.

First, in 2016 Champine *et al.* [4] reported new data for the ^{169}Tm$(n,2n)^{168}$Tm and ^{169}Tm$(n,3n)^{167}$Tm reactions between 17 and 22 MeV incident neutron energy. Shortly afterwards, Gooden *et al.* [5] published data for the ^{169}Tm$(n,3n)^{167}$Tm reaction between 23.5 and 30.5 MeV. Finally, Soter *et al.* [6] concentrated on the ^{169}Tm$(n,2n)^{168}$Tm reaction from threshold to 15 MeV. In the work of Champine *et al.* and Soter *et al.*, the ^{2}H$(d,n)^{3}$He reaction was used, while the work of Gooden *et al.* employed the ^{3}H$(d,n)^{4}$He reaction. All three experiments were performed at the Tandem Laboratory of the Triangle Universities Nuclear Laboratory (TUNL) [7]. They employed the well-known activation technique, i.e., after irradiation of the natural, mono-isotopic thulium samples, the induced γ-ray activity was measured with HPGe detectors of known efficiency at TUNL's low-background counting facility. For each transition of interest, published γ-ray intensities I_γ are necessary to convert the measured γ-ray counts into activity of the reaction product.

As stated already, the work of Champine *et al.* used the ^{2}H$(d,n)^{3}$He reaction as a neutron source. At the high deuteron energies needed to produce neutrons above 17 MeV, neutrons from the deuteron break-up reaction on structural materials of the deuterium gas cell and the deuterium gas itself create a substantial contamination of the monoenergetic neutron flux from the ^{2}H$(d,n)^{3}$He reaction, resulting in large corrections to the ^{169}Tm$(n,2n)^{168}$Tm cross-section data. The uncertainty in these corrections dominate the overall uncertainty of the ^{169}Tm$(n,2n)^{168}$Tm data reported in Ref. [4], limiting their importance compared to the already existing literature data in this energy range. It should be pointed out, however, that the ^{169}Tm$(n,3n)^{167}$Tm cross-section data, the major con-

* sfinch@tunl.duke.edu

TABLE I. Relevant nuclear data for the $(n,2n)$ and $(n,3n)$ cross-section determination of ^{169}Tm [4, 12–14]. Note that both ^{169}Tm and ^{197}Au are monoisotopic, having natural abundance of 100%.

Reaction	Threshold (MeV)	Half-life (d)	E_γ (keV)	I_γ (%)
^{169}Tm$(n,2n)^{168}$Tm	8.082	93.1 (2)	184.295 (2)	18.15 (16)
			198.251 (2)	54.49 (16)
			447.515 (3)	23.98 (11)
			815.989 (5)	50.95 (16)
^{169}Tm$(n,3n)^{167}$Tm	14.963	9.25 (2)	207.801 (5)	41.9(16)[a]
^{197}Au$(n,2n)^{196}$Au	8.114	6.1669 (6)	355.73 (5)	87(3)

[a] This value is the result of a new measurement from Ref. [4], while all other values are from Refs. [12–14].

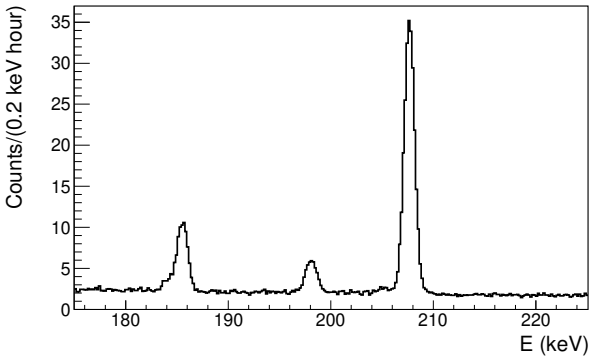

FIG. 1. Measured γ-ray spectrum at $E_n = 20.15$ MeV. The 184.295 and 198.251 keV transitions from the ^{169}Tm$(n,2n)^{168}$Tm reaction and the 207.801 keV transition from the ^{169}Tm$(n,3n)^{167}$Tm reaction may be clearly seen, and are easily distinguished using the high resolution of the HPGe detector. The 184.295 keV transition was not utilized in this work due to contamination by the naturally occurring background γ ray at 185.715 keV, resulting from the α decay of ^{235}U in the HPGe detector shielding.

tent of the work of Champine *et al.*, are not affected by the so-called deuteron break-up neutrons due to the high reaction threshold of 15.0 MeV.

In order to provide higher quality data for the ^{169}Tm$(n,2n)^{168}$Tm reaction in the 15 to 21 MeV incident neutron energy range, the present work used the ^{3}H$(d,n)^4$He reaction as monoenergetic neutron source. Because of its large Q-value of +17.6 MeV, deuteron break-up reactions are not an issue. As a by-product, cross-section data for the ^{169}Tm$(n,3n)^{167}$Tm reaction were obtained as well. Because the present work is a continuation and extension of the work of Soter *et al.* [6], using the same experimental setup, except for the ^{3}H$(d,n)^4$He neutron source reaction, and the same data-acquisition and data-analysis procedures, only a very brief description is given in the following Sec. II. The main emphasis is on the new results and their comparison to existing data and model and evaluations presented in Sec. III. Finally, Sec. IV provides a brief summary and concluding remarks.

II. EXPERIMENTAL SETUP, DATA-ACQUISITION AND ANALYSIS

The neutron activation technique [8, 9] was used to measure the ^{169}Tm$(n,2n)^{168}$Tm and ^{169}Tm$(n,3n)^{167}$Tm cross sections. A tritiated titanium foil was bombarded by deuteron beams provided by the model FN tandem accelerator at TUNL to produce monoenergetic neutron beams via the ^{3}H$(d,n)^4$He reaction at 12 energies between 14.8 and 21.1 MeV. The tritiated titanium target is described in Ref. [10]. Thulium foils of 7/16" diameter and 0.1 mm thickness were positioned at a distance of 2.5 cm from the end of the tritiated titanium foil. They were sandwiched between two gold foils of the same diameter as the thulium foils and thickness of 0.025 mm in order to use the ^{197}Au$(n,2n)^{196}$Au [11] reaction as neutron fluence monitor. Unique foils were used for each neutron energy due to the long ^{168}Tm half-life. The irradiation times increased from approximately two hours at 14.8 MeV to approximately eight hours at 21.1 MeV to account for the decrease of both the neutron yield from the ^{3}H$(d,n)^4$He reaction and the ^{169}Tm$(n,2n)^{168}$Tm cross section.

After irradiation, the foils were γ-ray counted on one of three different HPGe detectors of either 55% or 60% relative efficiency (compared to a 3" x 3" NaI detector). These detectors all have similar specifications (n-type Ortec HPGe detectors with a thin beryllium window) and utilize the same data acquisition system. Only small differences in the crystal size differentiate the three detectors. Long counting periods were required to accumulate statistics on ^{168}Tm ($t_{1/2} = 93.1$ d), and the use of only one HPGe detector would have severely limited the counting throughput. In order to reduce γ-ray summing effects, the foils were positioned at a distance of 5 cm from the front face of the HPGe detector. The same procedure was followed in the previous work [6]. Table I provides relevant information on the spectroscopic data needed to compute the cross sections of interest using the activation formulae (1) and (2) of Ref. [6] with the γ-ray yields, the measured HPGe detector efficiency obtained from a mixed γ-ray source [15] of known activity, containing 10 isotopes ranging from ^{241}Am (55.9 keV) to ^{88}Y (1836.1 keV), and applying small corrections for self-absorption, finite-geometry and summing effects.

III. RESULTS AND COMPARISON TO PREVIOUS DATA AND EVALUATIONS

Figure 2 shows the available experimental data for the ^{169}Tm$(n,2n)^{168}$Tm cross section from threshold up to 24 MeV in comparison to the commonly used nuclear data evaluations JEFF-3.3 [16], JENDL-4.0 [17], IRDFF-II [11] and ENDF/B-VIII.0 [18]. Here, we concentrate on neutron energies between 15 and 21 MeV, the energy range of the present data (blue circles). In contrast to the 14 MeV energy region, the previously existing data above 15 MeV are less abundant and exhibit smaller deviations from each other. The present data follow the trend established by the data sets of Veeser *et*

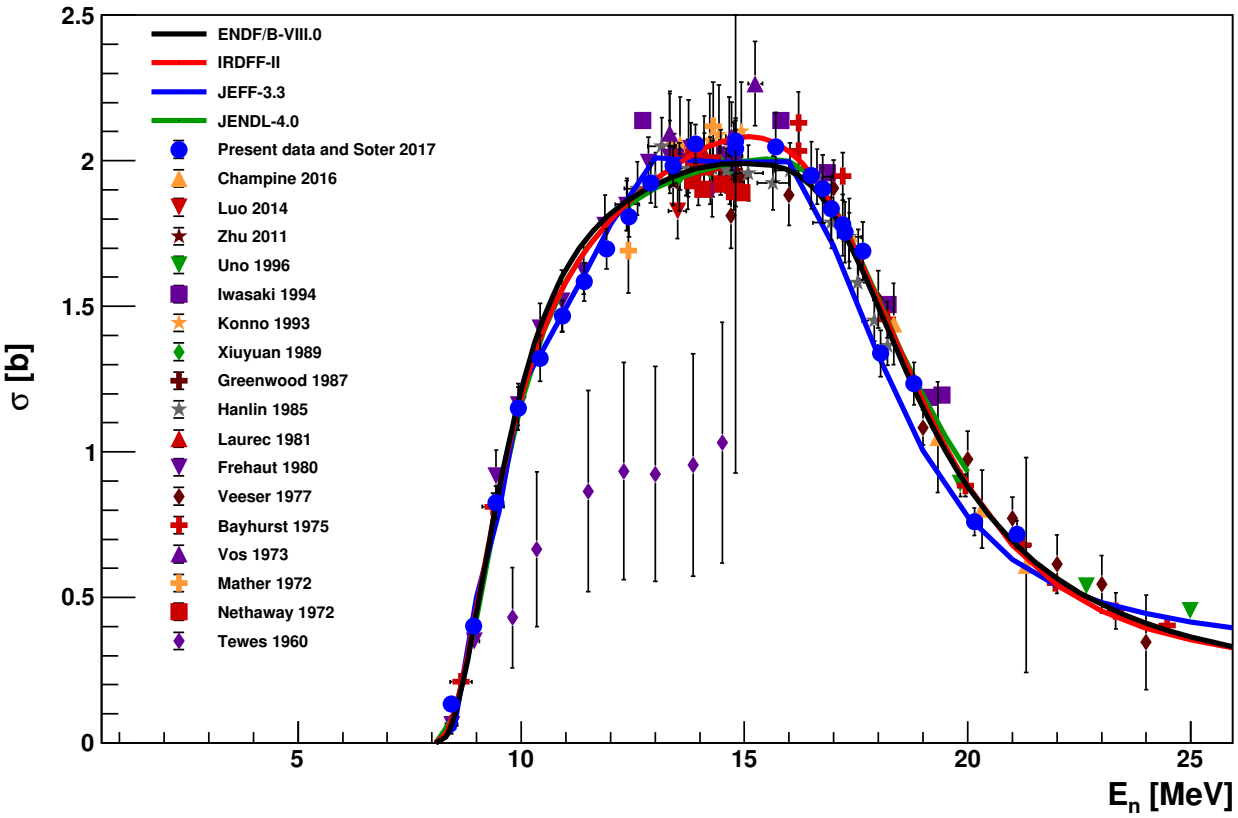

FIG. 2. (Color online) The present measurements of the ^{169}Tm$(n,2n)^{168}$Tm cross section compared to previous measurements and evaluations. Only measurements spanning multiple neutron energies are shown.

al. [19] and Hanlin et al. [20], while the datum of Bayhurst *et al.* [21] just below 17.5 MeV is clearly somewhat high, as is one of the two data points of Ref. [21] near 16 MeV. Our data also clearly show the improved accuracy achieved in the present work compared to the very recent work of Champine *et al.*, which utilized the ^{2}H$(d,n)^{3}$He neutron source reaction with its deuteron breakup-neutron contamination and associated fairly large correction uncertainty. The datum of Uno *et al.* [22] near 20 MeV follows the trend of our data, while the data of Iwasaki *et al.* [23] near 18 and 19.5 MeV are clearly too high.

Table II provides our results in numerical form. Here, the first column gives the mean neutron energy and associated energy spread. The second column presents the ^{197}Au$(n,2n)^{196}$Au cross section values used to obtain the cross-section results of interest, followed by our ^{169}Tm$(n,2n)^{168}$Tm cross-section results and their uncertainties in the third column. The total uncertainty in our ^{169}Tm$(n,2n)^{168}$Tm data varies between 5.6 and 6.5%, which includes uncertainties from the nuclear data inputs. These nuclear data uncertainties include the ^{197}Au$(n,2n)^{196}$Au reference cross section and γ-ray intensities, which contribute an uncertainty of 3.6-4.8%. The remaining experimental uncertainty varies from 4.3 to 4.6%, and is governed by the uncertainty in the γ-ray detection efficiency (3.1%), coincidence summing correction (2.5%), and counting statistics. A detailed uncertainty budget is shown in Table III. In addition to the sources of uncertainty, the correlation between uncertainties at different incident neutron energies is provided. We note that the largest sources of uncertainty, the γ-ray intensities, the HPGe detector efficiency, and coincidence summing correction, are highly or fully correlated between measurements. Although three different HPGe detectors were used, all detectors were calibrated using the same γ-ray source and procedure.

Concentrating on the comparison of the ^{169}Tm$(n,2n)^{168}$Tm cross-section data to the standard nuclear data evaluations above 15 MeV, we note that shifting the JEFF-3.3 evaluation to a higher energy by approximately 100 keV would result in a much better representation of the experimental data. The other three evaluations, JENDL-4.0, IRDFF-II, and ENDF/B-VIII.0, are in very close agreement to each other above 12 MeV. The energy range below 15 MeV has already been discussed in Ref. [6]. Overall, IRDFF-II seems to provide the best representation of the experimental ^{169}Tm$(n,2n)^{168}$Tm cross-section data in the entire energy range from threshold to 25 MeV.

The reason why we have obtained more ^{169}Tm$(n,2n)^{168}$Tm cross-section data in the 17 MeV neutron energy region than below and above this energy is related to the ^{169}Tm$(n,3n)^{167}$Tm reaction. Figure 3 shows the available experimental cross-section data for the ^{169}Tm$(n,3n)^{167}$Tm re-

TABLE II. Reported cross section measurements on ^{169}Tm, and the ^{197}Au$(n,2n)^{196}$Au reference cross section utilized, taken from IRDFF-II [11]. The reported uncertainty on the neutron energy represents the spread of the beam. The 198.251 keV transition from the decay of ^{168}Tm was used to produce the present results.

E_n (MeV)	^{197}Au$(n,2n)$ (mb)	^{169}Tm$(n,2n)$ (mb)	^{169}Tm$(n,3n)$ (mb)
14.8 ± 0.06	2164.5 ± 22.3	2042.8 ± 114	
15.7 ± 0.11	2163.5 ± 42.7	2046.9 ± 119	
16.5 ± 0.11	2100.8 ± 46.0	1949.6 ± 115	53.2 ± 3.9
16.75 ± 0.11	2060.0 ± 45.5	1903.4 ± 117	147.7 ± 10.8
16.95 ± 0.11	2019.1 ± 44.5	1835.9 ± 110	196.3 ± 14.3
17.2 ± 0.11	1957.8 ± 40.8	1779.1 ± 106	208.6 ± 15.0
17.25 ± 0.11	1944.0 ± 44.5	1754.6 ± 104	285.7 ± 20.4
17.65 ± 0.10	1821.0 ± 35.8	1689.9 ± 99.7	492.5 ± 34.6
18.05 ± 0.10	1679.4 ± 32.9	1338.2 ± 79.0	600.9 ± 42.7
18.8 ± 0.10	1397.3 ± 27.2	1234.3 ± 72.8	851.5 ± 59.9
20.15 ± 0.10	965.0 ± 28.2	760.0 ± 48.0	1040.8 ± 76.8
21.1 ± 0.10	756.6 ± 24.9	717.4 ± 47.0	1269.4 ± 96.2

TABLE III. Uncertainty budget for the present measurements. In addition to the individual sources of uncertainty, the correlation between individual neutron energies is provided.

Uncertainty	(%)	Correlation
^{197}Au cross section	1.0-3.3	
^{196}Au γ-ray intensity	3.45	1
^{168}Tm γ-ray intensity	0.29	1
^{167}Tm γ-ray intensity	3.82	1
^{168}Tm Half-life	0.21	1
^{167}Tm Half-life	0.21	1
Counting statistics	1.0-2.4	0
Detector efficiency	3.1	0.7
Coincidence summing	2.5	1
Source geometry and Self-absorption of γ rays	$<$0.5	1
Target mass	$<$0.1	1
Activation times	$<$0.5	0
Neutron flux fluctuation	$<$0.5	0

action from threshold to 30 MeV in comparison to our data (blue circles) in the 16.5 to 21 MeV energy range. Our data are in good agreement with the very recent data of Champine *et al.* [4] and all the other previous experimental data below 21 MeV, except for the two data of Bayhurst *et al.* [21] near 20 and 21 MeV. As noticed already for the ^{169}Tm$(n,2n)^{168}$Tm reaction, the more than 40 years old data of Veeser *et al.* [19] are in nice agreement with our data, which are presented in numerical form in the 4th column of Table II. Here, the individual contributions to the overall uncertainty associated with our data is similar to those discussed already for the ^{169}Tm$(n,2n)^{168}$Tm reaction. The total uncertainty is 7.0-7.6%, which includes a 5.5-6.1% contribution from the nuclear data inputs (the reference cross section and γ-ray intensities). The remaining experimental uncertainty is 4.4-4.7%. The ^{169}Tm$(n,3n)^{167}$Tm cross section is now very well determined in the RIF energy region up to approximately 18 MeV, an energy region more easily accessible in ICF shots at NIF than the higher energy RIF neutrons.

Turning now to the evaluation we note that the JEFF-3.3 evaluation is in disagreement with all experimental data below 20 MeV. In contrast to the ^{169}Tm$(n,2n)^{168}$Tm reaction, the IRDFF-II evaluation is in excellent agreement with the ^{169}Tm$(n,3n)^{167}$Tm data up to almost 25 MeV, while the ENDF/B-VIII.0 evaluation is somewhat low in the 18 MeV energy region. Above 21 MeV, the highest neutron energy used in the present work, all evaluations shown provide lower cross-section values than found in the recent work of Gooden *et al.* [5].

As the present data, combined with the previously published ^{169}Tm$(n,2n)^{169}$Tm data [6], spans two reaction thresholds and is all taken in a self-consistent manner, a valuable comparison may be made to theory models. This comparison was performed using the available models in TALYS [24]. Of the reaction parameters available, the level density model used was found to have the most relevant impact on the ^{169}Tm$(n,2n)^{169}$Tm and ^{169}Tm$(n,3n)^{169}$Tm cross sections. TALYS's default level densities are the constant temperature plus Fermi gas model [25] or the back-shifted Fermi gas model with a normalization factor for the average radiative width of $\Gamma_\gamma = 0.9$ [26]. Calculations using these two level densities are shown by the orange and green curves in Fig. 4, respectively. The best fit to our data was found using the recent microscopic level density, calculated using a the temperature dependent Hartree-Fock-Bogoliubov plus Gogny force, from Hilaire's combinatorial tables [27], shown by the purple curve in Fig. 4. Hilaire's microscopic model fits our data very well, and is a marked improvement over the Fermi gas models. This warrants a further investigation using measured reaction cross section data at vastly different atomic numbers.

IV. SUMMARY AND CONCLUSION

The ^{169}Tm$(n,2n)^{168}$Tm cross-section data obtained in the present work are a continuation of the work of Soter *et al.* [6] to extend the highest neutron energy from 15 to 21 MeV. The present data together with the previous data of Soter *et al.* present a comprehensive data set from threshold to 21 MeV. This has never been accomplished in any $(n,2n)$ experiments to date. The data of Bayhurst *et al.* [21] on many nuclei have been the "gold standard", but they have a gap between approximately 9 and 13 MeV, although they extend beyond 21 MeV, the highest energy in our present work. The advantage of a large and comprehensive data set is the fact that the size of potential systematic effects is common to all individual data points, making it easier for an evaluator to interpret the data as opposed to data sets from different sources and covering smaller energy ranges. The present data are in very good agreement with the ENDF/B-VIII.0 evaluation.

The present ^{169}Tm$(n,3n)^{167}$Tm cross-section data in the energy range between 16.5 and 21 MeV provide an accurate database to help interpreting RIF neutron yields at NIF. Our data are in excellent agreement with the data of Veeser *et al.* [19], supporting the observation that the ENDF/B-VIII.0 evaluation predicts slightly lower cross-section values than ob-

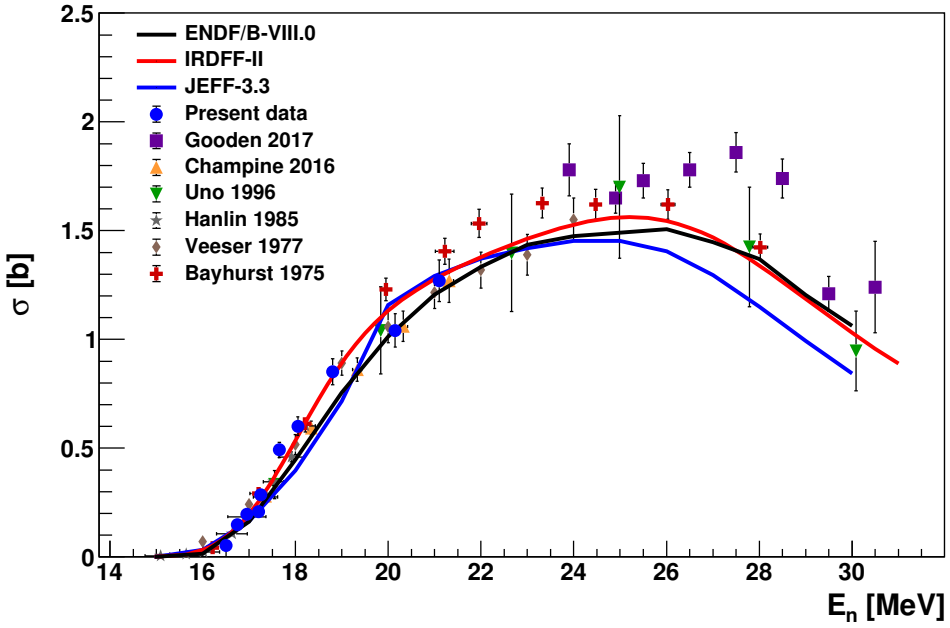

FIG. 3. (Color online) The present measurements of the ^{169}Tm$(n,3n)^{167}$Tm cross section compared to previous measurements and evaluations.

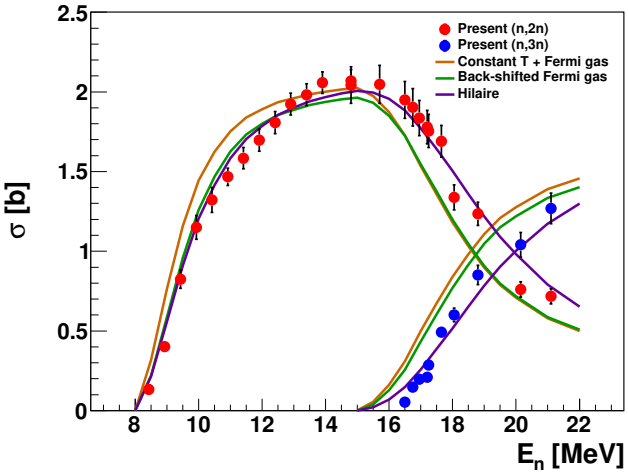

FIG. 4. (Color online) The present measurements of the ^{169}Tm$(n,2n)^{168}$Tm and ^{169}Tm$(n,3n)^{167}$Tm cross sections compared to different TALYS models. See text for a discussion of the models.

tained in our present work between 17.5 and 19 MeV, in contrast to the IRDFF-II evaluation which describes our data very well in the entire energy range investigated. Once higher energy RIF neutrons become available at NIF, it would be important to extend the ^{169}Tm$(n,3n)^{167}$Tm cross-section measurements to cover the energy range between 25 and 30 MeV, where experimental data are scarce and discrepant.

ACKNOWLEDGMENTS

This work was supported in part by the National Nuclear Security Administration under grant no. DE-NA0002936 and DE-NA0003884, and the U.S. Department of Energy, Office of Nuclear Physics, under grant no. DE-FG02-97ER41033. J. Soter acknowledges support from the NSF Research Experience for Undergraduate (REU) students program, under grant no. NSF-PHY-1461204.

[1] J. Lindl, O. Landen, J. Edwards, and E. Moses, Phys. Plasmas **21**, 020501 (2014).
[2] J. Frenje *et al.*, Nucl. Fusion **53**, 043014 (2013).
[3] A. C. Hayes, M. E. Gooden, E. Henry, G. Jungman, J. B. Wilhelmy, R. S. Rundberg, C. Yeamans, G. Kyrala, C. Cerjan, D. L. Danielson, J. Daligault, C. Wilburn, P. Volegov, C. Wilde, S. Batha, T. Bredeweg, J. L. Kline, G. P. Grim, E. P. Hartouni, D. Shaughnessy, C. Velsko, W. S. Cassata, K. Moody, L. F. Berzak Hopkins, D. Hinkel, T. Dppner, S. Le Pape, F. Graziani, D. A. Callahan, O. A. Hurricane, and D. Schneider, Nat. Phys. **16**, 432 (2020).
[4] B. Champine, M. E. Gooden, Krishichayan, E. B. Norman, N. D. Scielzo, M. A. Stoyer, K. J. Thomas, A. P. Tonchev, W. Tornow, and B. S. Wang, Phys. Rev. C **93**, 014611 (2016).
[5] M. E. Gooden, T. A. Bredeweg, B. Champine, D. C. Combs, S. Finch, A. Hayes-Sterbenz, E. Henry, Krishichayan, R. Rundberg, W. Tornow, J. Wilhelmy, and C. Yeamans, Phys. Rev. C **96**, 024622 (2017).
[6] J. Soter, M. Bhike, S. W. Finch, Krishichayan, and W. Tornow, Phys. Rev. C **96**, 064619 (2017).

[7] https://www.tunl.duke.edu/.

[8] A. P. Tonchev, C. T. Angell, M. Boswell, A. S. Crowell, B. Fallin, S. Hammond, C. R. Howell, A. Hutcheson, H. J. Karwowski, J. H. Kelley, R. S. Pedroni, W. Tornow, J. A. Becker, D. Dashdorj, J. Kenneally, R. A. Macri, M. A. Stoyer, C. Y. Wu, E. Bond, M. B. Chadwick, J. Fitzpatrick, T. Kawano, R. S. Rundberg, A. Slemmons, D. J. Vieira, and J. B. Wilhelmy, Phys. Rev. C **77**, 054610 (2008).

[9] M. Bhike, B. Fallin, M. E. Gooden, N. Ludin, and W. Tornow, Phys. Rev. C **91**, 011601(R) (2015).

[10] C. Bhatia, S. W. Finch, M. E. Gooden, and W. Tornow, Phys. Rev. C **87**, 011601(R) (2013).

[11] A. Trkov, P. Griffin, S. Simakov, L. Greenwood, K. Zolotarev, R. Capote, D. Aldama, V. Chechev, C. Destouches, A. Kahler, C. Konno, M. Kotl, M. Majerle, E. Malambu, M. Ohta, V. Pronyaev, V. Radulovi, S. Sato, M. Schulc, E. imekov, I. Vavtar, J. Wagemans, M. White, and H. Yashima, Nucl. Data Sheets **163**, 1 (2020).

[12] C. M. Baglin, Nucl. Data Sheets **90**, 431 (2000).

[13] C. M. Baglin, Nucl. Data Sheets **111**, 1807 (2010).

[14] H. Xiaolong, Nucl. Data Sheets **108**, 1093 (2007).

[15] Eckert & Ziegler Isotope Products, 24937 Ave Tibbitts, Valencia, CA 91355.

[16] A. J. M. Plompen *et al.*, Eur. Phys. J. A **56**, 181 (2020).

[17] K. Shibata *et al.*, J. Nucl. Sci. Technol. **48**, 1 (2011).

[18] D. Brown *et al.*, Nucl. Data Sheets **148**, 1 (2018), special Issue on Nuclear Reaction Data.

[19] L. R. Veeser, E. D. Arthur, and P. G. Young, Phys. Rev. C **16**, 1792 (1977).

[20] L. Han-Lin, Z. W. Rong, and F. P. Guo, Nucl. Sci. Eng. **90**, 304 (1985), https://doi.org/10.13182/NSE85-3.

[21] B. P. Bayhurst, J. S. Gilmore, R. J. Prestwood, J. B. Wilhelmy, N. Jarmie, B. H. Erkkila, and R. A. Hardekopf, Phys. Rev. C **12**, 451 (1975).

[22] Y. Uno, S. Meigo, S. Chiba, F. Fukahori, Y. Kasugai, O. Iwamoto, P. Siegler, and Y. Ikeda, in *9th International Symposium on Reactor Dosimetry* (Prague, 1996) p. 465.

[23] S. Iwasaki, S. Matsuyama, T. Ohkubo, M. Sakuma, and M. Kitamura, in *Conf. on Nuclear Data for Sci. and Techn.*, Vol. 1 (Gatlinburg, 1994) p. 305.

[24] O. Bersillon, F. Gunsing, E. Bauge, R. Jacqmin, and S. Leray, eds., *TALYS-1.0* (EDP Sciences, Nice, France, 2008).

[25] A. Koning, S. Hilaire, and S. Goriely, Nuclear Physics A **810**, 13 (2008).

[26] P. Demetriou and S. Goriely, Nuclear Physics A **695**, 95 (2001).

[27] S. Hilaire, M. Girod, S. Goriely, and A. J. Koning, Phys. Rev. C **86**, 064317 (2012).